

Histone Deacetylase Inhibitors Influence Chemotherapy Transport by Modulating Expression and Trafficking of a Common Polymorphic Variant of the ABCG2 Efflux Transporter

Agnes Basseville¹, Akina Tamaki¹, Caterina Ierano¹, Shana Trostel¹, Yvona Ward², Robert W. Robey¹, Ramanujan S. Hegde³, and Susan E. Bates¹

Abstract

Histone deacetylase inhibitors (HDI) have exhibited some efficacy in clinical trials, but it is clear that their most effective applications have yet to be fully determined. In this study, we show that HDIs influence the expression of a common polymorphic variant of the chemotherapy drug efflux transporter ABCG2, which contributes to normal tissue protection. As one of the most frequent variants in human ABCG2, the polymorphism Q141K impairs expression, localization, and function, thereby reducing drug clearance and increasing chemotherapy toxicity. Mechanistic investigations revealed that the ABCG2 Q141K variant was fully processed but retained in the aggresome, a perinuclear structure, where misfolded proteins aggregate. In screening for compounds that could correct its expression, localization, and function, we found that the microtubule-disrupting agent colchicine could induce relocalization of the variant from the aggresome to the cell surface. More strikingly, we found that HDIs could produce a similar effect but also restore protein expression to wild-type levels, yielding a restoration of ABCG2-mediated specific drug efflux activity. Notably, HDIs did not modify aggresome structures but instead rescued newly synthesized protein and prevented aggresome targeting, suggesting that HDIs disturbed trafficking along microtubules by eliciting changes in motor protein expression. Together, these results showed how HDIs are able to restore wild-type functions of the common Q141K polymorphic isoform of ABCG2. More broadly, our findings expand the potential uses of HDIs in the clinic. *Cancer Res*; 72(14); 3642–51. ©2012 AACR.

Introduction

ATP-binding cassette transporters (ABC) are energy-dependent transporters involved in absorption, distribution, and excretion of drugs and in cancer drug resistance (1). ABCG2 is a member of the G subfamily of human ABC transporters and is a half-transporter that must dimerize for function (2). ABCG2 transports numerous anticancer agents including mitoxantrone, etoposide, topotecan, and tyrosine kinase inhibitors (3). In addition, ABCG2 substrates include antivirals, antibiotics, and toxins, highlighting the apparent role of ABCG2 transporters in normal tissue protection, including the blood–brain and maternal–fetal barriers. It has also been observed that ABCG2 may play a protective role with respect to exposure to smoke or dietary carcinogens (4, 5).

Authors' Affiliations: ¹Medical Oncology Branch, ²Cell and Cancer Biology Branch, Center for Cancer Research, National Cancer Institute, NIH; and ³Cell Biology and Metabolism Branch, SIPT, NICHHD, NIH, Bethesda, Maryland

Note: Supplementary data for this article are available at Cancer Research Online (<http://cancerres.aacrjournals.org/>).

Corresponding Author: Susan E. Bates, Medical Oncology Branch, National Cancer Institute, NIH, 7000 Rockville Pike, Bethesda, MD 20892. Phone: 301-402-1357; Fax: 301-402-1608; E-mail: sebates@helix.nih.gov

doi: 10.1158/0008-5472.CAN-11-2008

©2012 American Association for Cancer Research.

The most studied ABCG2 polymorphism is the nonsynonymous single-nucleotide polymorphism (SNP) C421A, which results in a glutamic acid to lysine substitution at amino acid 141 (Q141K), localized in the ATP-binding domain. C421A allele frequency is high in the Japanese and Chinese population (26%–35%), whereas it is 10% to 12% for Caucasians and less than 1% in the African population (3). ABCG2 harboring Q141K has impaired protein expression, incomplete trafficking to the plasma membrane, and decreased function. Clinically, the Q141K polymorphism has been linked to reduced clearance of some ABCG2 substrate drugs including diflomotecan, irinotecan, topotecan, gefitinib, rosuvastatin, atorvastatin, fluvastatin, simvastatin, and sulfasalazine (6). In addition to its impact on pharmacokinetics, the Q141K SNP has recently been linked to at least 10% of all gout cases, as the decreased ABCG2 function reduces urate elimination (7).

Because of the clinical significance of the Q141K polymorphism in anticancer drug pharmacokinetics and potential involvement in carcinogenesis, we studied processing and trafficking of the intracellular trapped variant protein and ways of rescuing Q141K ABCG2 to restore it to its wild-type (WT) phenotype. Previous studies have shown that the defective folding and trafficking of some ABC transporter variants of P-glycoprotein (Pgp) or the cystic fibrosis transmembrane conductance regulator (CFTR) could be partially rescued by ligands that act as pharmacologic chaperones to correct the

folding defect (8–11). These compounds function by promoting interactions between protein domains during folding. In the same way, previous studies in our laboratory showed that mitoxantrone, a substrate of ABCG2, had the ability to rescue ABCG2 mutant protein (12). Here, we screened various compounds: mitoxantrone, the microtubule disruptor colchicine, and 4 different histone deacetylase (HDAC) inhibitors. HDAC proteins were first discovered for their involvement in gene regulation via histone deacetylation. It appears, however, that HDACs have broader activities than expected and have been shown, for example, to deacetylate various transcription factors or proteins involved in cell growth, death, or cellular transport. In recent years, clinical development of HDAC inhibitors (HDI) has emerged in cancer therapy, and several classes of HDIs have been explored in preclinical models and reached the clinic (13, 14).

We found that HDIs induced ABCG2 variant rescue and we attempted to elucidate the mechanism of action of HDIs on ABCG2 processing.

Materials and Methods

Cell culture

Flp-In-293 cells were obtained from Invitrogen. WT and Q141K ABCG2 sublines were created by transfection of the pcDNA5/FRT/V5-His-TOPO vector (Invitrogen) expressing WT or Q141K ABCG2 into Flp-In-293 cells, an HEK293 subline bearing a single integrated Flp Recombination Target site (Invitrogen), according to the manufacturer's instructions. Cells were authenticated by STR-DNA technology (RADIL) after establishment of different ABCG2 sublines and then aliquoted and frozen. After being thawed, cells were cultured in minimum essential medium supplemented with 10% FBS, 100 µg/mL Hygromycin B (Invitrogen), 2 mmol/L glutamine, and 100 U/L penicillin/streptomycin (BioFluids).

Chemicals

Mitoxantrone and cycloheximide were purchased from Sigma; panobinostat, vorinostat, and 17AAG from ChemieTek; valproic acid from EMD4Biosciences; and tubastatin from BioVision. Romidepsin was obtained from the Developmental Therapeutics Program of National Cancer Institute (NCI)/NIH (Bethesda, MD).

Immunofluorescence

Immunofluorescence was conducted as previously described (12), and the following primary antibodies were used: anti-ABCG2 BXP-21 (Kamiya Biomedical Company); anti-giantin, anti-TGN46, anti-HDAC6, anti- γ -tubulin, or anti-vimentin (Abcam). Nuclei were stained with 4',6-diamidino-2-phenylindole (DAPI) and cells were visualized on a Zeiss LSM510 META laser scanning microscope (Zeiss), equipped with an Apo63 \times 1.4 oil DIC II objective.

RNA extraction and quantitative PCR

Isolation of total RNA was carried out with High Pure RNA Isolation Kit (Roche). cDNA synthesis was conducted from 1 µg RNA in a reverse transcriptase reaction using MMLV enzyme and random hexamers (Invitrogen). cDNA ABCG2 was ampli-

fied in a LightCycler Thermocycler by LightCycler TaqMan Master Mix (Roche Diagnostics) and probes from Roche Universal ProbeLibrary. The expression levels of ABCG2 were normalized with rRNA.

Western blot

Blots were probed with the following primary antibodies: anti-ABCG2, anti-GAPDH (American Research Products, Inc.); anti-BiP (BD Biosciences); anti-Hsp90, anti-Hsc70 (Stressgen); anti-Hsp70 (Cell Signaling); anti-acetyl-histone H3 (Santa Cruz); and anti-dynamitin (Abcam). Secondary antibody (LI-COR Biosciences) was used to visualize quantifiable results with the Odyssey System (LI-COR Biosciences).

Endo H and PNGase F assay

Cell lysates were incubated with *N*-glycosidase F (PNGase F) or endoglycosidase H (Endo H; ProZyme) at 37°C for 3 hours and immunoblotted.

Processing experiments

Cells were incubated for 24 hours at 37°C with 3 µmol/L MG132 (EMD4Biosciences), 10 nmol/L bafilomycin, or 2 mmol/L 3-methyladenine (Sigma). Proteins were then extracted and immunoblotted.

Flow cytometry

Flow cytometry examining ABCG2 with anti-ABCG2 antibody 5D3 (eBioscience) was carried out as previously described (12). Cells were analyzed with a FACSort flow cytometer with CellQuest software (BD Biosciences). Transport studies were conducted as previously described (12) with 200 nmol/L BODIPY-Prazosin (Invitrogen) with or without 10 µmol/L fumitremorgin C (FTC; Developmental Therapeutics Program NCI/NIH), an ABCG2 inhibitor. The rate of cell death was measured via Annexin V/PI assay (BD Pharmingen), according to the manufacturer's protocol.

siRNA

Cells were transfected with untargeted siRNA or siRNA against dynamitin (SMARTpool, Dharmacon), according to the manufacturer's protocol. After 48 hours, immunoblotting was conducted to determine the efficacy of the knockdown.

Statistical analysis

The Student *t* test was carried out for each experiment represented with a bar graph and asterisks indicate a significant difference ($P < 0.05$) compared with control.

Results

Determination of Q141K ABCG2 trafficking

Flp-In-293 cells were selected for this study, as one copy of the vector is known to insert at a unique specific site, resulting in comparable RNA levels. To evaluate ABCG2 WT and Q141K variant localization in cells, immunofluorescent experiments were carried out. As previously reported (15–17), we saw that Q141K ABCG2 proteins had incomplete trafficking and cytoplasmic retention, whereas WT proteins were mainly localized

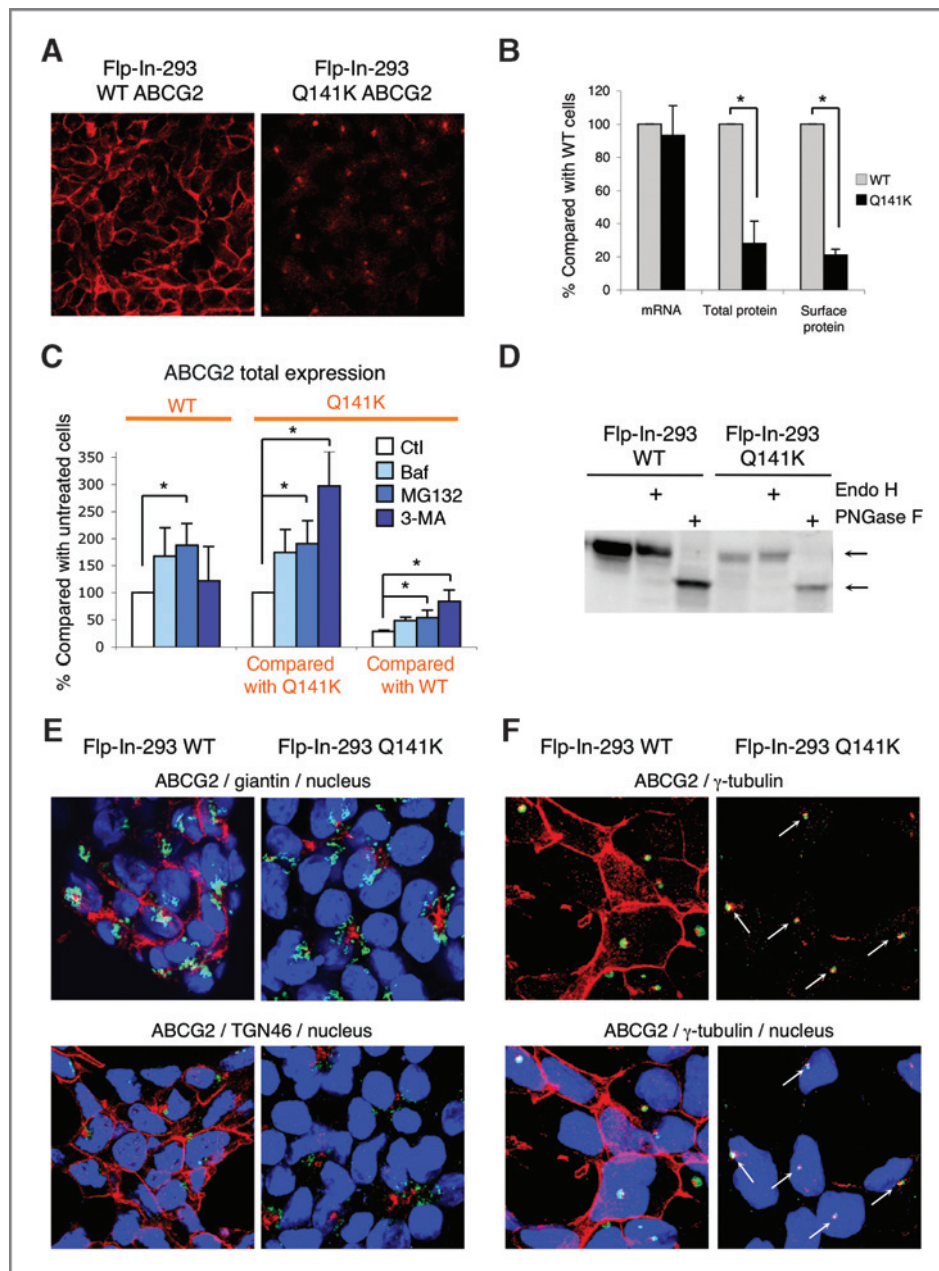


Figure 1. Determination of Q141K ABCG2 localization, processing, and degradation pathways. **A**, ABCG2 was detected by immunofluorescence in Flp-In-293 cells. **B**, mRNA and protein were detected by quantitative PCR (qPCR) and immunoblotting, and ABCG2 surface expression was determined by flow cytometry. **C**, Flp-In-293 cells were incubated for 24 hours with bafilomycin (Baf; 10 nmol/L), MG132 (3 μ mol/L), or 3-methyladenine (3-MA; 2 mmol/L), and ABCG2 expression was determined by immunoblotting. **D**, enzymatic deglycosylation was conducted with PNGase F and Endo H, then ABCG2 was detected by immunoblotting. **E** and **F**, Flp-In-293 cells showing nuclei (blue), ABCG2 (red), and Golgi marker (giantin; **E**, top), *trans*-Golgi marker (TGN46; **E**, bottom), or γ -tubulin (**F**) in green. White arrows point to the site of aggresome. Ctl, control.

in the cell membrane (Fig. 1A). Also noted was staining of large aggregates of proteins, suggesting that the Q141K ABCG2 variant was accumulated in a localized cellular area.

Although Q141K and WT ABCG2 mRNA levels were equal, variant protein levels were 4-fold lower, suggesting that a posttranslational mechanism regulates expression (Fig. 1B). Accordingly, the Q141K variant showed 5-fold decreased surface expression compared with WT.

We hypothesized that Q141K variant underexpression was due to protein degradation. To explore whether Q141K ABCG2 was degraded by the ubiquitin-proteasome, the endosome-lysosome, or the autophagic pathways, we treated the cells with the proteasome inhibitor MG132; bafilomycin A1, which inhi-

bits lysosomal degradation; and 3-methyladenine, which inhibits autophagosome formation. Bafilomycin and MG132 treatment increased total protein expression (between 150% and 180%) for WT and Q141K protein (Fig. 1C). These data suggest that in normal processing, a small portion of WT and Q141K ABCG2 are degraded via the proteasomal pathway, whereas the fully processed proteins that reach the surface are degraded by the lysosome, as observed for other transmembrane proteins (18). Interestingly, the inhibition of the autophagic pathway induced a 3-fold increase in Q141K ABCG2 levels but barely affected WT protein expression. This indicates that autophagy is the main posttranslational mechanism, leading to a loss of Q141K variant expression. To support this

conclusion, we induced autophagy by starvation or rapamycin and observed a further decrease in variant levels after 16- and 24-hour treatments (Supplementary Fig. S1). We also observed that a higher proportion of Q141K variant is ubiquitinated than in the WT protein (Supplementary Fig. S2). Moreover, whereas ABCG2 is ubiquitinated when it is targeted to the proteasome, it is not when it is targeted to the autophagosome.

To examine the processing of Q141K ABCG2, whole-cell lysates from Flp-In-293 cells were deglycosylated with PNGase F and Endo H. ABCG2 contains a polysaccharide chain on asparagine 596 (19). PNGase F removes these glycans at any stage of processing, whereas Endo H cleaves immature oligosaccharides. No change in molecular mass was observed after Endo H digestion (Fig. 1D), suggesting that both WT and Q141K ABCG2 were completely processed and not retained in the endoplasmic reticulum.

We next evaluated the localization of the retained ABCG2 variant in Flp-In-293 cells by immunofluorescent colocalization experiments. Two Golgi markers were used: giantin, a *cis*/medial Golgi marker, and TGN46, a *trans*-Golgi network marker (20). Results showed that Q141K was not retained in Golgi (Fig. 1E). We then asked whether Q141K ABCG2 proteins were retained in aggresomes. These structures, localized around the centrosome, are inclusion bodies where misfolded proteins aggregate (21). In Fig. 1F, we observed that the intracellular-retained ABCG2 variant was mainly localized around γ -tubulin, a centrosome marker, a finding consistent with localization in the aggresome (22). Thus, the major fraction of Q141K variant accumulated in the aggresomes. While WT ABCG2 was mainly on the membrane, it was also discernable in the aggresome.

Together, these results indicated that WT ABCG2 was normally processed and mainly localized in the cytoplasmic membrane, whereas a small fraction underwent proteasome degradation or entrapment in the aggresome. The Q141K ABCG2 variant reached its mature form but was mainly sequestered in the aggresome and degraded via autophagy. A small fraction of variant also reached the surface or underwent proteasomal degradation.

Impact of mitoxantrone on ABCG2 protein expression and localization

Studies in CFTR or Pgp have identified compounds that act as pharmacologic chaperones to promote folding and trafficking of mature proteins to the cell surface (8–11). We previously showed that mitoxantrone increased the processing of an ABCG2 mutant (12). The effects of mitoxantrone were thus assayed in Q141K ABCG2 variant trafficking. We first determined whether mitoxantrone exposure induced ABCG2 expression in Flp-In-293 cells by using quantitative PCR, immunoblotting, and flow cytometry (Fig. 2A). Treatment with 5 μ M mitoxantrone for 24 hours caused a small increase in WT and Q141K total ABCG2 expression (around 125% for mRNA and 120% for protein compared with untreated cells). Surface expression showed a 160% induction in WT cells and a 250% induction in Q141K cells (Fig. 2A). The subcellular localization of ABCG2 following mitoxantrone was evaluated by immunofluorescent confocal microscopy. Q141K variant

showed a marked homogeneous staining pattern, with loss of aggresome localization, whereas Flp-In-293 WT cells showed no change (Fig. 2B). Finally, ABCG2 net efflux was determined by fluorescence-activated cell sorting (FACS) in Flp-In-293 WT and Q141K cells after mitoxantrone treatment (Fig. 2C). Pretreatment with mitoxantrone for 24 hours caused a weak increase of substrate net efflux (113% and 128% for WT and Q141K ABCG2, respectively).

Taken together, these results suggested that mitoxantrone stopped variant aggresome targeting, but recruitment to the cell surface was still incomplete.

Impact of HDIs on ABCG2 protein expression, localization, and function

We previously reported the ability of HDIs to increase ABCG2 mRNA levels (23, 24). Four HDIs were evaluated for their impact on ABCG2 expression and processing. Romidepsin affects primarily class I HDACs, whereas panobinostat, vorinostat, and valproic acid are more broad-spectrum HDIs (13). We first determined the effect of HDIs on ABCG2 mRNA and protein expression in the ABCG2 Flp-In-293 sublines treated for 24 hours with 46 nmol/L romidepsin, 100 nmol/L panobinostat, 10 μ M vorinostat, or 1 mmol/L valproic acid (Fig. 3A). Following treatment with romidepsin, panobinostat, and vorinostat, ABCG2 mRNA levels showed a 250% to 350% increase, presumably due to transcriptional regulation following altered histone acetylation (23). Total and surface protein expressions were similarly increased (210%–310% for WT ABCG2 and 260%–375% for Q141K ABCG2). Valproic acid induced the weakest effect on mRNA and protein ABCG2 expression (150%–200% increase). The same experiments carried out in mock Flp-In-293 cells showed that endogenous ABCG2 was not expressed, even after HDI treatment (Supplementary Fig. S3), assuring that we only studied the transfected ABCG2.

Localization of ABCG2 was examined by confocal microscopy after HDI treatment. Again, basal plasma membrane localization of WT far exceeded that in Flp-In-293 Q141K cells, where ABCG2 was localized in aggresomes (Fig. 3B). After exposure to HDIs, WT ABCG2 showed a minimal change in localization, whereas a dramatic change was seen for Q141K ABCG2. Panobinostat, vorinostat, and especially romidepsin induced a significant decrease in ABCG2 inside the cell and increased staining along the cell surface. In Fig. 3C, we observed in detail that in romidepsin-treated Flp-In-293 Q141K cells, the aggresome-localized ABCG2 had almost disappeared in favor of a strong surface localization. ABCG2-specific efflux was then determined by FACS after HDI treatment in Flp-In-293 WT and Q141K cells. In Flp-In-293 WT cells, 24-hour HDI pretreatment led to a weak increase of substrate net efflux compared with untreated cells (110%–120%). However, the change in transport ability following exposure to the HDIs in Flp-In-293 Q141K cells was notably higher: 200% for romidepsin, 163% for panobinostat, and 210% for vorinostat, compared with untreated Flp-In-293 Q141K cells (Fig. 3D). Increased Q141K ABCG2 function was confirmed by a cell death assay using the ABCG2 substrate, pheophorbide A (Fig. 3E). Indeed, Flp-In-293 Q141K cells pretreated for 24 hours with

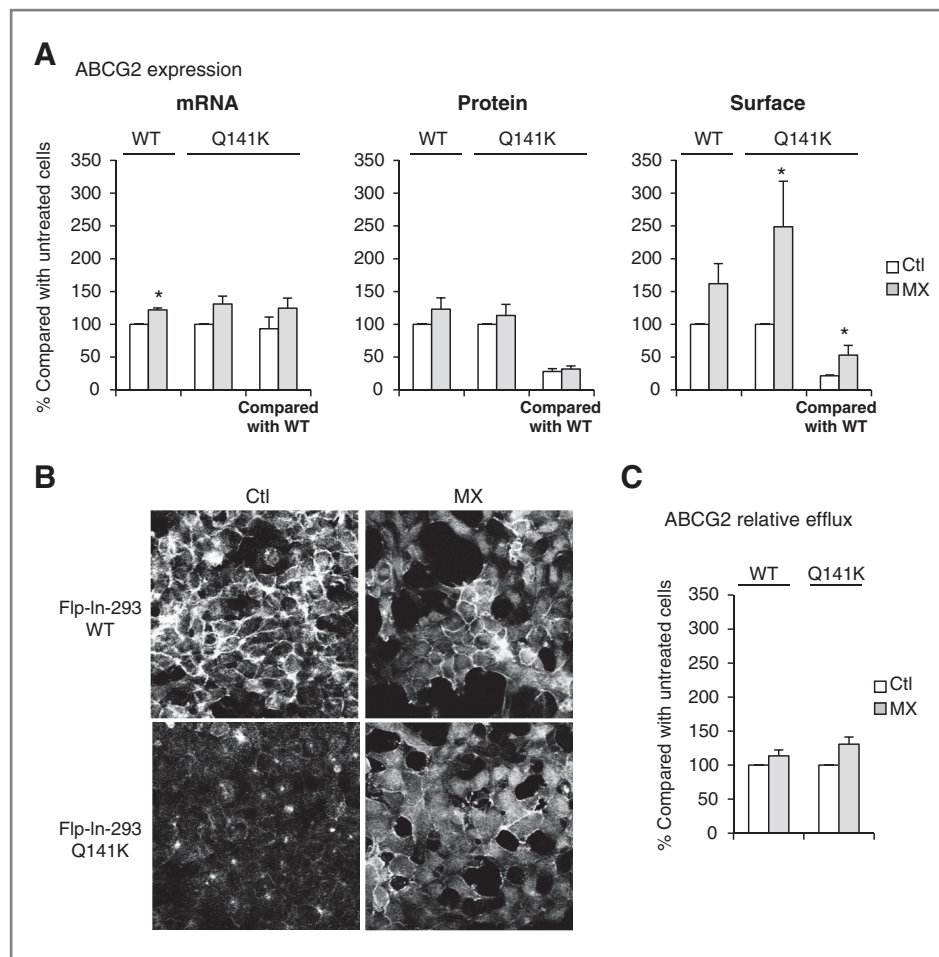


Figure 2. Impact of mitoxantrone on ABCG2 protein expression and localization. A, Flp-In-293 cells were submitted to 24-hour exposure to 5 μ mol/L mitoxantrone (MX) and then ABCG2 mRNA, protein, and surface expression were detected by qPCR, immunoblotting, and flow cytometry, respectively. Q141K mRNA, total protein, and surface protein expression was 93%, 28%, and 21%, respectively, of WT ABCG2. B, ABCG2 was shown by confocal microscopy in Flp-In-293 WT and Q141K cells after 24-hour treatment with mitoxantrone. C, ABCG2 relative efflux was determined by FACS after 24-hour treatment with mitoxantrone. Q141K relative efflux was 39.5% of WT ABCG2. Ctl, control.

romidepsin showed a decrease in cell death after pheophorbide A treatment compared with cells not pretreated. Notably, it appears that WT is also rendered more efficient after HDI treatment in the cell death assay, although the efflux assay was not sufficiently sensitive to detect this increasing WT ABCG2 efflux (saturating levels).

Altogether, these results indicate that romidepsin, vorinostat, and panobinostat induced an increase in WT and Q141K ABCG2 expression that was associated with an improved trafficking to the cell surface in the Q141K variant. The increase also came with a gain of Q141K ABCG2 function, indicating that the surface variant was functional.

Transcriptional effects of HDIs on Q141K ABCG2 rescue

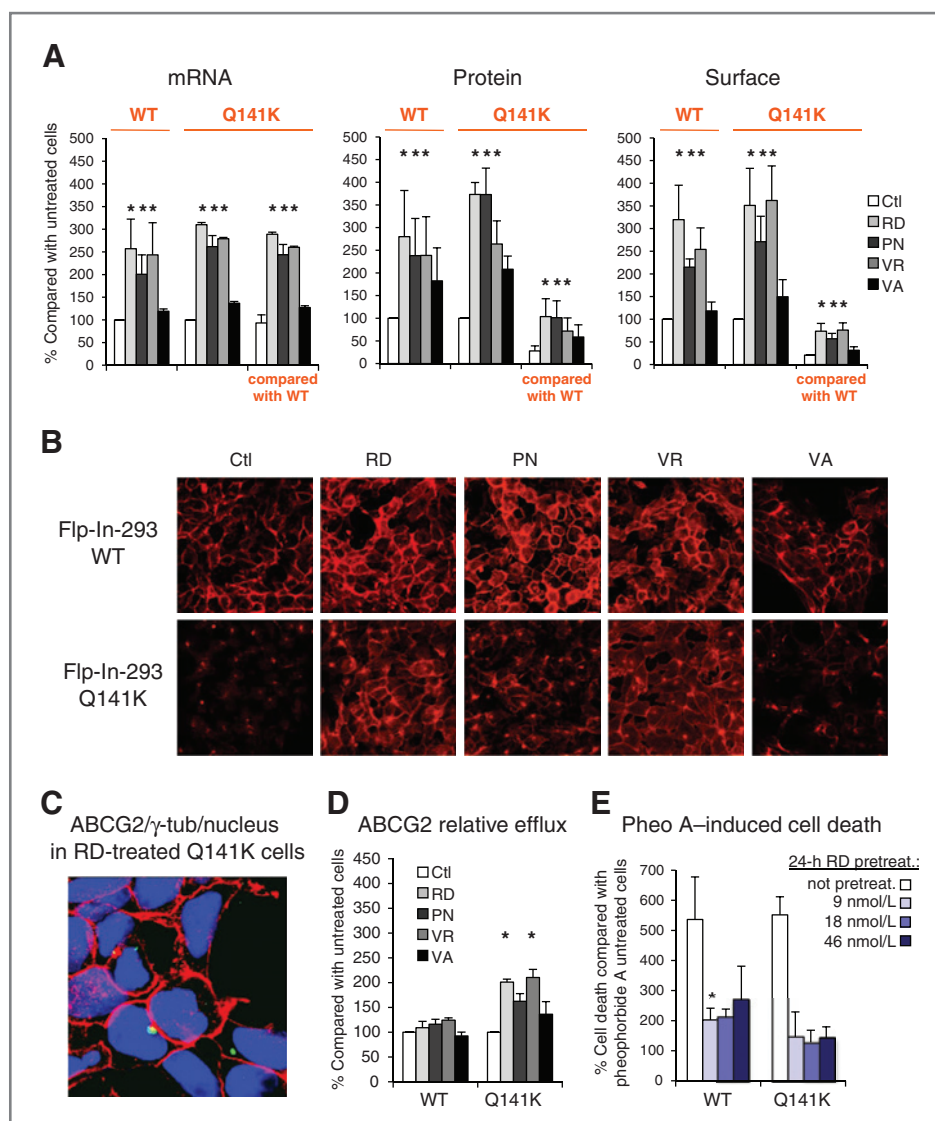
Our goal was to determine the mechanism by which HDI treatment leads to improvement of ABCG2 mutant trafficking. We first determined whether the increased ABCG2 expression on the cell surface required new protein synthesis. We treated cells simultaneously with HDIs and cycloheximide, an inhibitor of protein biosynthesis. We verified that cycloheximide does not affect the histone and α -tubulin acetylation, induced by HDIs (Supplementary Fig. S4). We then observed, in both Flp-In-293 WT and Q141K cells, that the mitoxantrone- and HDI-induced increases in surface expression were abolished by

inhibition of protein synthesis (Fig. 4A), and the same results were obtained with the transcription inhibitor actinomycin D (Supplementary Fig. S5). These experiments indicated that HDI- and mitoxantrone-induced rescue require transcription events. Whereas mitoxantrone did not induce increased protein expression, the protein synthesis inhibitor cycloheximide abrogated the mitoxantrone-induced variant surface increase. This suggests that mitoxantrone only modified the trafficking of the neosynthesized ABCG2 and would not act on Q141K ABCG2 already trapped in the aggresome.

We also monitored the effect of romidepsin on mRNA and surface expression of ABCG2 over time. We observed that the drug-induced increase in mRNA expression of the 2 proteins was only detectable after 12 hours, and that the increased ABCG2 surface expression appeared subsequently, after 16 hours of treatment (Fig. 4B). These results support the conclusion that the transporter cell surface rescue was more likely due to a gene transcription-related event than to a direct acetylation-induced cytoplasmic event.

We compared the data from mitoxantrone and HDI effect on Q141K ABCG2 localization and function. We noted that mitoxantrone induced a relocalization of the variant in a homogeneous cytoplasmic pattern and weakly on the plasma membrane, linked to a weak increase in ABCG2 function. HDIs

Figure 3. Impact of HDIs on WT and Q141K ABCG2 protein expression, localization, and function. A, ABCG2 mRNA, total and surface protein were, respectively, quantified by qPCR, immunoblotting, and FACS analysis in Flp-In-293 WT and Q141K cells following 24-hour exposure to 46 nmol/L romidepsin (RD), 100 nmol/L panobinostat (PN), 10 μ mol/L vorinostat (VR), or 1 mmol/L valproic acid (VA). B, ABCG2 repartition was visualized in cells by immunofluorescence after 24-hour HDI exposure. C, ABCG2 and γ -tubulin were observed in Q141K cells after 24-hour RD treatment (magnified example). Tub, tubulin. D, ABCG2 net efflux was determined by FACS after 24-hour treatment with HDIs. E, cells were pretreated or not with RD dilutions for 24 hours, then treated for 24 hours with pheophorbide A (pheo A; 1 μ mol/L for WT and 0.5 μ mol/L for Q141K cells), and cell death was measured by flow cytometry. Ctl, control.



induced mainly Q141K ABCG2 trafficking to the membrane, accompanied by a greater increase in protein function. From these results, we hypothesized that HDIs induced not only ABCG2 expression but also genes encoding proteins that enhanced ABCG2 folding and/or trafficking.

To find an ABCG2-folding partner, we focused on chaperone protein expression after 24-hour HDI treatment. We did not observe changes in Bip, Hsc70, Hsp70, or Hsp90 expression (Supplementary Fig. S6), suggesting that HDI-mediated correction of trafficking cannot be ascribed to induction of these chaperones.

Nontranscriptional mechanisms of HDIs inducing Q141K ABCG2 rescue

Considering ABCG2 acetylation as a possible mechanism of rescue, we immunoprecipitated ABCG2 and immunoblotted for acetylated lysine but saw no effect of HDIs on the transporter acetylation state (data not shown).

We observed that Q141K ABCG2 was retained in aggresomes. The formation of aggresomes begins with the coalition of small, unfolded protein aggregates, which are dispersed in the periphery of the cytoplasm and travel on microtubules toward the microtubule-organizing center region. There they remain as stable particulate structures entangled with intermediate filaments such as vimentin, until degradation by autophagy or by the proteasome (21). In several models, HDAC6 has also been involved in retrograde transport by binding both misfolded proteins and the motor protein dynein, which then transports the misfolded protein-HDAC6 complexes toward aggresomes by traveling along microtubules (21, 25, 26).

We asked whether HDIs disturbed aggresome maintenance. In Fig. 5A, we observed that the microtubule-organizing center (centrosome) and vimentin were not disrupted by exposure to romidepsin, indicating maintenance of the aggresome structure.

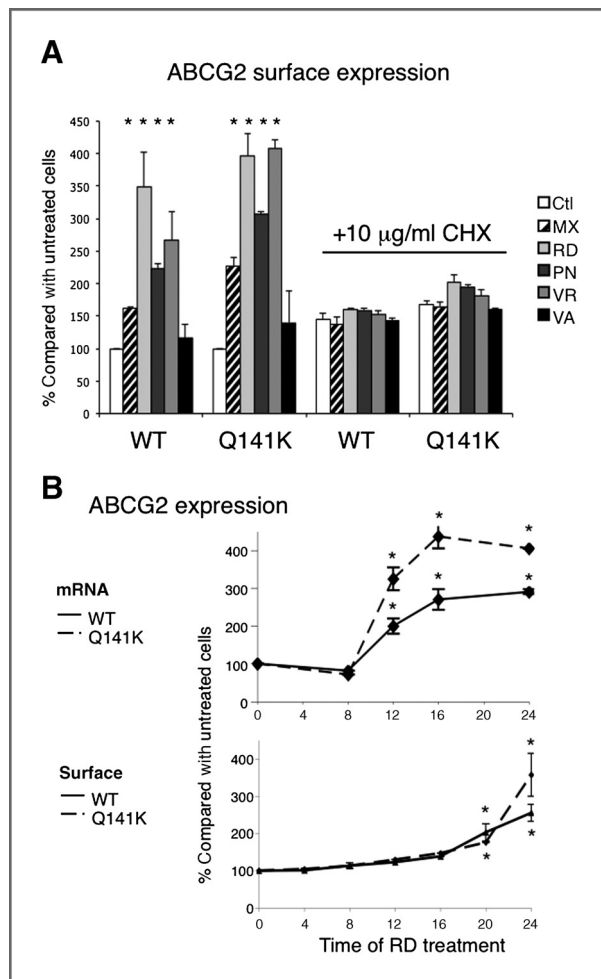


Figure 4. Transcriptional effects of HDIs on ABCG2 Q141K rescue. A, quantification of ABCG2 surface expression by FACS in Flp-In-293 WT and Q141K cells after 24-hour exposure to mitoxantrone (MX) and HDIs in presence or absence of cycloheximide (CHX). B, time course of ABCG2 mRNA (top) and surface expression (bottom) in Flp-In-293 cells during romidepsin (RD) treatment (46 nmol/L) was realized by qPCR and FACS using the 5D3 antibody, respectively. Ctl, control; PN, panobinostat; VA, valproic acid; VR, vorinostat.

We next examined the role of microtubules, known to be involved in retrograde transport, in ABCG2 localization. A previous study has shown that romidepsin did not alter the microtubule structure (27), but it is possible that HDIs disturb the trafficking along microtubules. To study the involvement of microtubule retrograde transport in ABCG2 rescue, we used colchicine, a microtubule polymerization inhibitor. Surprisingly, immunofluorescent experiments showed that colchicine induced a dispersion of the ABCG2 variant aggregates and a relocalization of ABCG2 to the surface (Fig. 5B), much as observed with HDI treatment. Total ABCG2 expression was unchanged after colchicine treatment (Fig. 5C). On the basis of the colchicine results, we concluded that HDI-induced ABCG2 rescue could also involve inhibition of retrograde transport along microtubules.

We then asked how HDIs could disturb retrograde transport. To evaluate HDAC6 involvement in Q141K ABCG2 rescue, we treated Flp-In-293 Q141K cells with the HDAC6 inhibitor tubastatin (28). In Fig. 5D, we observed that the HDAC6 inhibition observed after 24-hour treatment with 2.5 μ mol/L tubastatin did not induce ABCG2 variant rescue. Moreover, cotreatment of tubastatin with romidepsin (class I HDI) did not induce an additional effect. No change was expected with the other HDIs, knowing that they already inhibit HDAC6. We concluded that HDAC6 inhibition was not involved in variant rescue. We then evaluated the involvement of the motor protein complex in ABCG2 rescue. It has been shown that overexpression of dynaminin induces the disruption of dynein from microtubules, leading to abrogation of aggresome formation (29). We studied dynaminin expression after HDI treatment and observed that romidepsin, panobinostat, and vorinostat, but not valproic acid, induced dynaminin overexpression (Fig. 5E). Knowing that valproic acid is the only HDI that does not induce ABCG2 rescue, these results suggest that HDIs might inhibit ABCG2 retrograde transport via dissociation of dynein from microtubules, due to dynaminin overexpression. To confirm these data, we conducted an siRNA assay to inhibit the expression of dynaminin, and we assessed the effect of HDIs on ABCG2 Q141K rescue after dynaminin knockdown. As shown in Fig. 5F, dynaminin knockdown blunted the effect of HDIs on Q141K ABCG2 rescue with a significant effect for romidepsin.

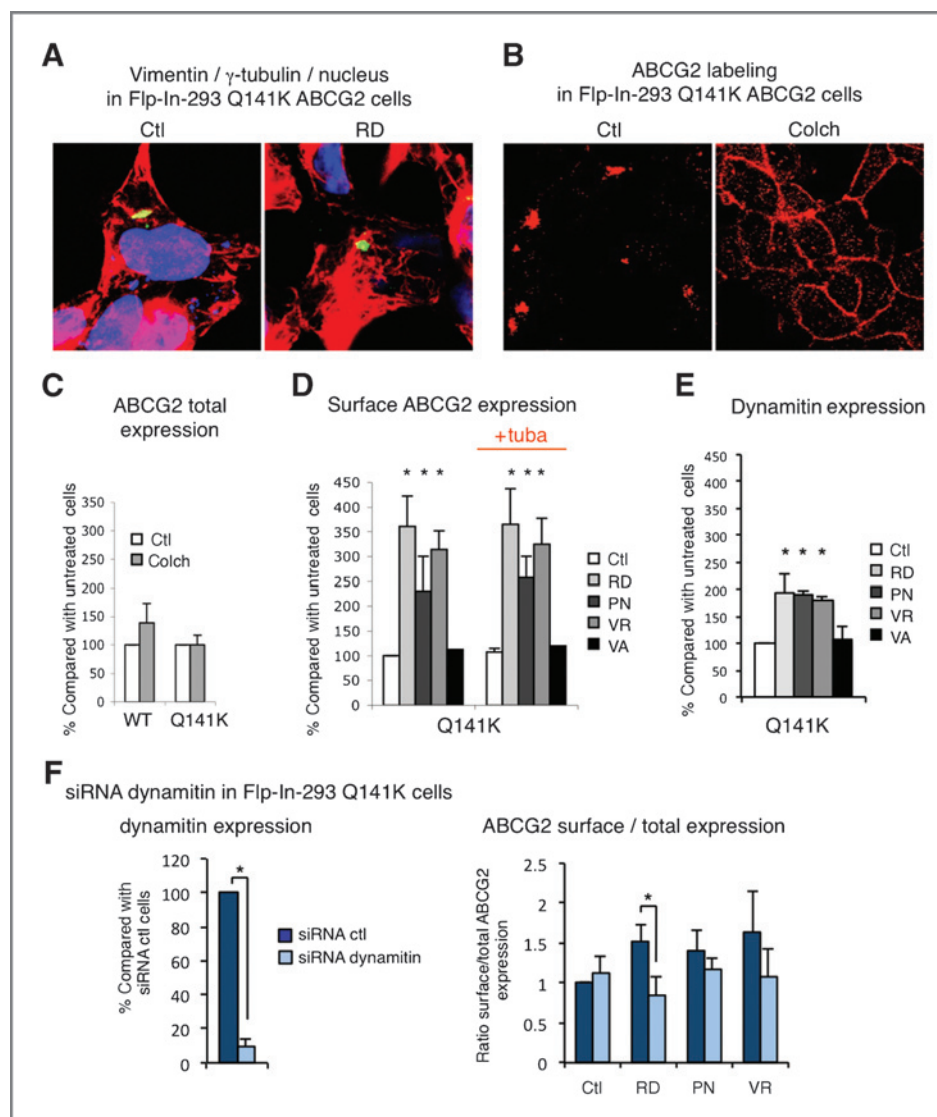
Discussion

We saw that the Q141K variant was retained in aggresomes and then degraded by the autophagic pathway. The aggresome was discovered by Johnston and colleagues (21) as a cellular area where misfolded undegraded CFTR molecules accumulate. They proposed that aggresome formation was a general response of cells, occurring when proteasome capacity is exceeded by misfolded protein production. Aggresome formation facilitates the capture of aggregated proteins by the autophagic pathway (30–33), which we observed to be the case for Q141K ABCG2. A previous study had shown in the same Flp-In-293 cell model that Q141K ABCG2 was subjected to ubiquitin-mediated proteasomal and lysosomal degradation, with a 2-fold increase in expression after treatment with both inhibitors (17). We also found that a fraction of ABCG2 variant was degraded via the proteasome and lysosome, with a 1.8- to 1.9-fold increase after inhibition. The authors concluded that it undergoes lysosomal and proteasomal degradations but did not explore the possibility of an autophagic pathway.

It is interesting to note that the expressed WT and Q141K ABCG2 variants are found in a fully mature form, contrary to what has been observed with other ABC transporters. For example, CFTR with the Δ F508 deletion results in a defectively folded protein that fails to mature and is rapidly degraded (34, 35). In the same way, only WT Pgp is processed in mature form, whereas some mutants are intracellularly retained in an immature form (36).

We sought to rescue Q141K ABCG2 trafficking using HDIs. The HDIs induced ABCG2 mRNA, total, and surface protein

Figure 5. Nontranscriptional effects of HDIs on ABCG2 Q141K rescue. **A**, vimentin and γ -tubulin localization were observed by confocal microscopy in Flp-In-293 Q141K cells after a 24-hour treatment with 46 nmol/L romidepsin (RD). **B**, the effect of colchicine (colch; 1 μ mol/L, 24 hours) on ABCG2 localization was determined by immunofluorescence in Flp-In-293 Q141K ABCG2 cells. **C**, ABCG2 total expression was quantified by immunoblot in Flp-In-293 WT and Q141K cells after 24-hour exposure to 1 μ mol/L colchicine. **D**, quantification of ABCG2 surface expression by FACS in Flp-In-293 Q141K cells after 24-hour exposure to HDIs in presence or absence of 2.5 μ mol/L tubastatin (tuba). **E**, quantitation of dynamitin expression by immunoblot after 24-hour treatment with HDIs. **F**, the knockdown of dynamitin was observed after 48-hour transfection in Q141K cells by immunoblotting (left). The effect of dynamitin knockdown was then assessed on ABCG2 Q141K protein expression (surface and total) after a subsequent 24-hour HDI treatment. Ctl, control; PN, panobinostat; VA, valproic acid; VR, vorinostat.



expression with a conserved ratio for WT as for Q141K variant. More importantly, HDIs caused a strong relocalization of the Q141K variant from aggresome to cell surface and increased Q141K-mediated efflux. We sought to understand why these HDI-induced Q141K proteins, instead of accumulating in the aggresomes, were able to traffic to the cell surface. The rescue by the HDIs required protein neosynthesis and an approximate 16-hour delay. As suggested for mitoxantrone, these results imply that HDIs improve neosynthesized transporter folding rather than affecting the already aggresome-trapped variant. They also implicate an increase in trafficking mechanisms via transcription regulation rather than by a more immediate signaling or acetylation event. We observed that dynamitin was overexpressed, probably leading to the inhibition of retrograde transport via the disruption of dynein from microtubules. The partial inhibition of the HDI effect on ABCG2 rescue after dynamitin knockdown suggested that inhibition of retrograde transport is a part of HDI mechanism of action.

Other proteins involved in protein folding or trafficking might also be regulated. For example, Hutt and colleagues (37) have shown that suberoylanilide hydroxamic acid (SAHA)-induced rescue of CFTR variant was also mainly due to gene transcription regulation. Interestingly, they showed, by siRNA screen of all class I and II HDACs, that inhibition of HDAC7 restored CFTR trafficking and activity on cell surface. HDAC7 regulated a set of genes involved in CFTR folding, maturation, trafficking, and channel activation. HDAC1 inhibition also restored CFTR variant trafficking but not its function.

We observed that colchicine was also able to rescue Q141K ABCG2 trafficking. This drug, which inhibits microtubule polymerization, is already known to disrupt aggresome formation and retrograde transport (38). We deduced that HDIs similarly inhibit Q141K retrograde transport toward the aggresome, likely via dynamitin overexpression. HDIs might also directly inhibit HDACs involved in retrograde transport. For example, Kim and colleagues (39) recently showed that during

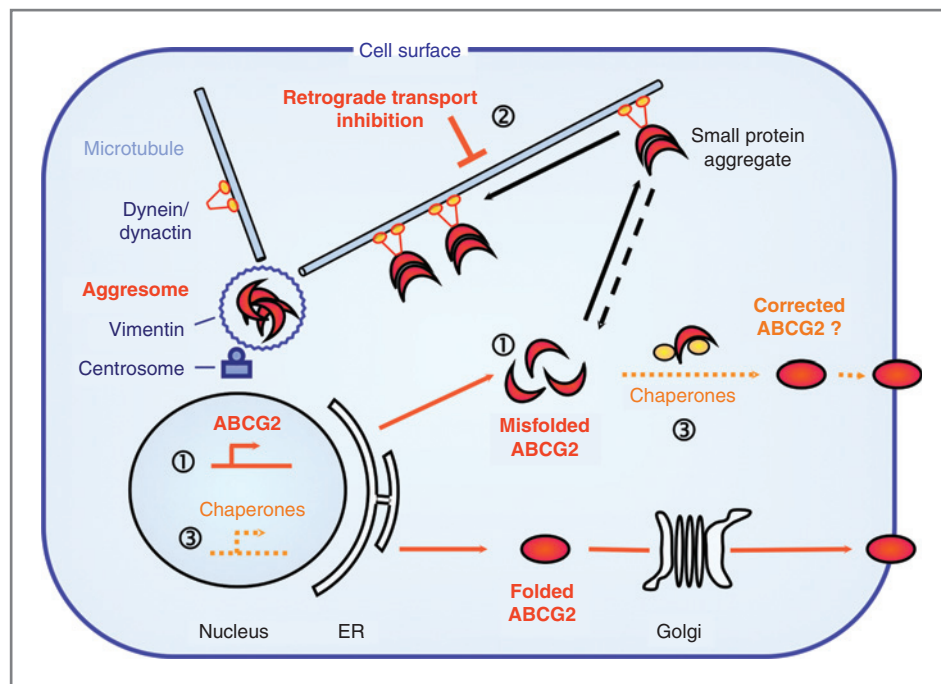


Figure 6. Proposed mechanism of multiple target HDI-mediated Q141K ABCG2 rescue. HDIs act on Q141K ABCG2 trafficking by inducing ABCG2 overexpression (1) and likely a trafficking/folding partner overexpression (3), as well as by inhibition of retrograde transport from cytoplasm to aggresome (2). ER, endoplasmic reticulum.

an inflammatory stimulus, HDAC1 competed with the adaptor proteins for binding to motor proteins that travel along the microtubules, impairing axonal transport in neurons. This suggests a new role for HDAC1 in protein trafficking. Nawrocki and colleagues (40) also showed that inhibition of HDAC6 led to disruption of the aggresomes, but our experiments suggested that this deacetylase was not involved in the Q141K ABCG2 rescue.

On the basis of our results, we propose a multipathway mechanism for HDI-induced Q141K ABCG2 rescue to surface (Fig. 6). HDIs induced Q141K ABCG2 surface localization by an increase in ABCG2 transcription coupled to dynactin overexpression, which reduced aggresome targeting by inhibition of dynein/microtubule retrograde transport. Other protein partners might also improve the neosynthesized variant folding and trafficking, as observed with the CFTR variant (37).

HDIs are promising anticancer agents. They were initially thought to simply reverse aberrant epigenetic changes associated with cancer, but it was soon observed that the inhibition of HDAC activity led to pleiotropic activities via various cellular and molecular pathways. These broad effects make it difficult to identify the key molecular events that determine the biologic response to HDIs. Here, we highlighted a new molecular mechanism, HDIs acting as "modulators of protein trafficking.

The use of molecules acting as "correctors" of variant protein processing and "potentiators" of variant protein activity, largely developed *in vitro*, has just shown its first clinical success. Ramsey and colleagues (41) observed in a phase III clinical trial that the CFTR potentiator ivacaftor, used to treat CFTR variant carriers, was associated with a sustained 17% relative improvement in lung function. These successful results highlight the potential of this emerging treatment strategy in the clinic and open doors to a new use of HDIs as ABCG2-defective variant

correctors to treat gout and imply that a chemoprevention strategy could be identified if ABCG2 were found to be important in carcinogenesis. Regardless of therapeutic relevance, this study offers insights into the processing of a protein of increasing importance in pharmacology, blood-brain barrier, and normal tissue protection.

Disclosure of Potential Conflicts of Interest

No potential conflicts of interest were disclosed.

Authors' Contributions

Conception and design: A. Basseville, A. Tamaki, C. Ierano, S.E. Bates
Development of methodology: A. Basseville, A. Tamaki, C. Ierano, S. Trostel, Y. Ward
Acquisition of data (provided animals, acquired and managed patients, provided facilities, etc.): A. Basseville, A. Tamaki, C. Ierano, Y. Ward, R.W. Robey
Analysis and interpretation of data (e.g., statistical analysis, biostatistics, computational analysis): A. Basseville, A. Tamaki, Y. Ward, R.S. Hegde, S.E. Bates
Writing, review, and/or revision of the manuscript: A. Basseville, A. Tamaki, Y. Ward, R.W. Robey, S.E. Bates
Administrative, technical, or material support (i.e., reporting or organizing data, constructing databases): A. Basseville, A. Tamaki, S. Trostel, Y. Ward
Study supervision: A. Tamaki, R.S. Hegde, S.E. Bates

Acknowledgments

The authors thank Drs. To and Polgar for the Flp-In-293 cell line establishment, and Julian Bahr for English editing.

Grant Support

This research was supported by the Intramural Research Program of the Center for Cancer Research, National Cancer Institute at NIH.

The costs of publication of this article were defrayed in part by the payment of page charges. This article must therefore be hereby marked *advertisement* in accordance with 18 U.S.C. Section 1734 solely to indicate this fact.

Received June 16, 2011; revised March 26, 2012; accepted March 27, 2012; published OnlineFirst April 3, 2012.

References

- Dean M, Hamon Y, Chimini G. The human ATP-binding cassette (ABC) transporter superfamily. *J Lipid Res* 2001;42:1007–17.
- Ozvegy C, Litman T, Szakács G, Nagy Z, Bates S, Váradi A, et al. Functional characterization of the human multidrug transporter, ABCG2, expressed in insect cells. *Biochem Biophys Res Commun* 2001;285:111–7.
- Robey RW, To KK, Polgar O, Dohse M, Fetsch P, Dean M, et al. ABCG2: a perspective. *Adv Drug Deliv Rev* 2009;61:3–13.
- van Herwaarden AE, Jonker JW, Wagenaar E, Brinkhuis RF, Schellens JH, Beijnen JH, et al. The breast cancer resistance protein (Bcrp1/Abcg2) restricts exposure to the dietary carcinogen 2-amino-1-methyl-6-phenylimidazo[4,5-b]pyridine. *Cancer Res* 2003;63:6447–52.
- van Herwaarden AE, Wagenaar E, Karnekamp B, Merino G, Jonker JW, Schinkel AH. Breast cancer resistance protein (Bcrp1/Abcg2) reduces systemic exposure of the dietary carcinogens aflatoxin B1, IQ and Trp-P-1 but also mediates their secretion into breast milk. *Carcinogenesis* 2006;27:123–30.
- Ni Z, Bikadi Z, Rosenberg MF, Mao Q. Structure and function of the human breast cancer resistance protein (BCRP/ABCG2). *Curr Drug Metab* 2010;11:603–17.
- Dehghan A, Kottgen A, Yang Q, Hwang SJ, Kao WL, Rivadeneira F, et al. Association of three genetic loci with uric acid concentration and risk of gout: a genome-wide association study. *Lancet* 2008;372:1953–61.
- Loo TW, Bartlett MC, Clarke DM. Rescue of folding defects in ABC transporters using pharmacological chaperones. *J Bioenerg Biomembr* 2005;37:501–7.
- Pedemonte N, Sonawane ND, Taddei A, Hu J, Zegarra-Moran O, Suen YF, et al. Phenylglycine and sulfonamide correctors of defective delta F508 and G551D cystic fibrosis transmembrane conductance regulator chloride-channel gating. *Mol Pharmacol* 2005;67:1797–807.
- Wang Y, Loo TW, Bartlett MC, Clarke DM. Modulating the folding of P-glycoprotein and cystic fibrosis transmembrane conductance regulator truncation mutants with pharmacological chaperones. *Mol Pharmacol* 2007;71:751–8.
- Loo TW, Bartlett MC, Clarke DM. Correctors promote folding of the CFTR in the endoplasmic reticulum. *Biochem J* 2008;413:29–36.
- Polgar O, Ierano C, Tamaki A, Stanley B, Ward Y, Xia D, et al. Mutational analysis of threonine 402 adjacent to the GXXXG dimerization motif in transmembrane segment 1 of ABCG2. *Biochemistry* 2010;49:2235–45.
- Bolden JE, Peart MJ, Johnstone RW. Anticancer activities of histone deacetylase inhibitors. *Nat Rev Drug Discov* 2006;5:769–84.
- Ma X, Ezzeldin HH, Diasio RB. Histone deacetylase inhibitors: current status and overview of recent clinical trials. *Drugs* 2009;69:1911–34.
- Mizuarai S, Aozasa N, Kotani H. Single nucleotide polymorphisms result in impaired membrane localization and reduced atpase activity in multidrug transporter ABCG2. *Int J Cancer* 2004;109:238–46.
- Morisaki K, Robey R, Ozvegy-Laczka C, Honjo Y, Polgar O, Steadman K, et al. Single nucleotide polymorphisms modify the transporter activity of ABCG2. *Cancer Chemother Pharmacol* 2005;56:161–72.
- Furukawa T, Wakabayashi K, Tamura A, Nakagawa H, Morishima Y, Osawa Y, et al. Major SNP (Q141K) variant of human ABC transporter ABCG2 undergoes lysosomal and proteasomal degradations. *Pharm Res* 2009;26:469–79.
- Turnbull EL, Rosser MF, Cyr DM. The role of the UPS in cystic fibrosis. *BMC Biochem* 2007;8:Suppl 1:S11.
- Diop N, Hrycyna C. N-linked glycosylation of the human ABC transporter ABCG2 on asparagine 596 is not essential for expression, transport activity, or trafficking to the plasma membrane. *Biochemistry* 2005;44:5420–9.
- Prescott AR, Lucocq JM, James J, Lister JM, Ponnambalam S. Distinct compartmentalization of TGN46 and beta 1,4-galactosyltransferase in HeLa cells. *Eur J Cell Biol* 1997;72:238–46.
- Johnston JA, Ward CL, Kopito RR. Aggresomes: a cellular response to misfolded proteins. *J Cell Biol* 1998;143:1883–98.
- Zheng Y, Jung MK, Oakley BR. Gamma-tubulin is present in *Drosophila melanogaster* and *Homo sapiens* and is associated with the centrosome. *Cell* 1991;65:817–23.
- To K, Polgar O, Huff L, Morisaki K, Bates S. Histone modifications at the ABCG2 promoter following treatment with histone deacetylase inhibitor mirror those in multidrug-resistant cells. *Mol Cancer Res* 2008;6:151–64.
- To KK, Robey R, Zhan Z, Bangiolo L, Bates SE. Upregulation of ABCG2 by romidepsin via the aryl hydrocarbon receptor pathway. *Mol Cancer Res* 2011;9:516–27.
- Kawaguchi Y, Kovacs JJ, McLaurin A, Vance JM, Ito A, Yao TP. The deacetylase HDAC6 regulates aggresome formation and cell viability in response to misfolded protein stress. *Cell* 2003;115:727–38.
- Corcoran LJ, Mitchison TJ, Liu Q. A novel action of histone deacetylase inhibitors in a protein aggresome disease model. *Curr Biol* 2004;14:488–92.
- Sandor V, Robbins AR, Robey R, Myers T, Sausville E, Bates SE, et al. FR901228 causes mitotic arrest but does not alter microtubule polymerization. *Anticancer Drugs* 2000;11:445–54.
- Hubbert C, Guardiola A, Shao R, Kawaguchi Y, Ito A, Nixon A, et al. HDAC6 is a microtubule-associated deacetylase. *Nature* 2002;417:455–8.
- Johnston JA, Illing ME, Kopito RR. Cytoplasmic dynein/dynactin mediates the assembly of aggresomes. *Cell Motil Cytoskeleton* 2002;53:26–38.
- Kopito RR. Aggresomes, inclusion bodies and protein aggregation. *Trends Cell Biol* 2000;10:524–30.
- Fortun J, Dunn WA Jr, Joy S, Li J, Notterpek L. Emerging role for autophagy in the removal of aggresomes in Schwann cells. *J Neurosci* 2003;23:10672–80.
- Iwata A, Christianson JC, Bucci M, Ellerby LM, Nukina N, Forno LS, et al. Increased susceptibility of cytoplasmic over nuclear polyglutamine aggregates to autophagic degradation. *Proc Natl Acad Sci U S A* 2005;102:13135–40.
- Chin LS, Olzmann JA, Li L. Parkin-mediated ubiquitin signalling in aggresome formation and autophagy. *Biochem Soc Trans* 2010;38:144–9.
- Lukacs GL, Mohamed A, Kartner N, Chang XB, Riordan JR, Grinstein S. Conformational maturation of CFTR but not its mutant counterpart (delta F508) occurs in the endoplasmic reticulum and requires ATP. *EMBO J* 1994;13:6076–86.
- Ward CL, Kopito RR. Intracellular turnover of cystic fibrosis transmembrane conductance regulator. Inefficient processing and rapid degradation of wild-type and mutant proteins. *J Biol Chem* 1994;269:25710–8.
- Loo TW, Clarke DM. Prolonged association of temperature-sensitive mutants of human P-glycoprotein with calnexin during biogenesis. *J Biol Chem* 1994;269:28683–9.
- Hutt DM, Herman D, Rodrigues AP, Noel S, Pilewski JM, Matteson J, et al. Reduced histone deacetylase 7 activity restores function to misfolded CFTR in cystic fibrosis. *Nat Chem Biol* 2010;6:25–33.
- Riley NE, Bardag-Gorce F, Montgomery RO, Li J, Lungo W, Lue YH, et al. Microtubules are required for cytokeratin aggresome (Mallory body) formation in hepatocytes: an *in vitro* study. *Exp Mol Pathol* 2003;74:173–9.
- Kim JY, Shen S, Dietz K, He Y, Howell O, Reynolds R, et al. HDAC1 nuclear export induced by pathological conditions is essential for the onset of axonal damage. *Nat Neurosci* 2010;13:180–9.
- Nawrocki ST, Carew JS, Pino MS, Highshaw RA, Andtbacka RH, Dunner K Jr, et al. Aggresome disruption: a novel strategy to enhance bortezomib-induced apoptosis in pancreatic cancer cells. *Cancer Res* 2006;66:3773–81.
- Ramsey BW, Davies J, McElvaney NG, Tullis E, Bell SC, Drevinek P, et al. A CFTR potentiator in patients with cystic fibrosis and the G551D mutation. *N Engl J Med* 2011;365:1663–72.

Cancer Research

The Journal of Cancer Research (1916–1930) | The American Journal of Cancer (1931–1940)

Histone Deacetylase Inhibitors Influence Chemotherapy Transport by Modulating Expression and Trafficking of a Common Polymorphic Variant of the ABCG2 Efflux Transporter

Agnes Basseville, Akina Tamaki, Caterina Ierano, et al.

Cancer Res 2012;72:3642-3651. Published OnlineFirst April 3, 2012.

Updated version Access the most recent version of this article at:
doi:[10.1158/0008-5472.CAN-11-2008](https://doi.org/10.1158/0008-5472.CAN-11-2008)

Supplementary Material Access the most recent supplemental material at:
<http://cancerres.aacrjournals.org/content/suppl/2012/04/03/0008-5472.CAN-11-2008.DC1.html>

Cited articles This article cites 41 articles, 14 of which you can access for free at:
<http://cancerres.aacrjournals.org/content/72/14/3642.full.html#ref-list-1>

Citing articles This article has been cited by 2 HighWire-hosted articles. Access the articles at:
<http://cancerres.aacrjournals.org/content/72/14/3642.full.html#related-urls>

E-mail alerts [Sign up to receive free email-alerts](#) related to this article or journal.

Reprints and Subscriptions To order reprints of this article or to subscribe to the journal, contact the AACR Publications Department at pubs@aacr.org.

Permissions To request permission to re-use all or part of this article, contact the AACR Publications Department at permissions@aacr.org.